International Deep Drawing Research Group
IDDRG 2009 International Conference
presented by John Tyson II, PE,
Trilion Quality Systems,
1-3 June 2009, Golden, CO, USA

YIELD CURVE DETERMINATION USING THE BULGE TEST COMBINED WITH OPTICAL MEASUREMENT

Dr. Stefan Keller[1], Dr. Walter Hotz[2], and Dr. Harald Friebe[3]

[1] Hydro Aluminium Research & Development
Georg-von-Boeselager-Straße 21, 53117 Bonn, Germany
E-mail: stefan.keller@hydro.com, Web page: www.hydro.com

[2] Novelis Innovation Centre
3960 Sierre, Switzerland
E-mail: walter.hotz@novelis.com, Web page: www.novelis.com

[3] GOM mbH
Mittelweg 7-8, 38106 Braunschweig, Germany
E-mail: info@gom.com, Web page: www.gom.com

ABSTRACT

Yield curves (true-stress vs. true-strain curves) describe a material's work-hardening behavior during forming and are thus indispensable for all FE forming simulations. The most common and, at the moment, only standardized test for yield curve determination is the tensile test. The tensile test, however, has the disadvantage that only a relatively small degree of deformation can be achieved before fracture occurs. This is caused by the uniaxial stress state.

Multiaxial stress states are present in nearly all industrial forming processes, resulting in a much higher degree of deformation than achieved in tensile tests. Therefore, for the simulation of such forming processes, an extrapolation of the measured yield curve is required but not permitted by metal physics. However, by using a hydraulic stretch-drawing test (i.e. bulge test) combined with an online strain measurement system, yield curves can be determined to a far higher degree of deformation than in tensile tests. This leads to a significantly improved description of the yield curve and makes extrapolation largely unnecessary.

To exploit the great potential of such a combined measurement system, GOM, Hydro and Novelis established a joint venture in 2004 and developed a method which facilitates the measurement of the pressure, dome height, dome curvature and the equivalent strain at the apex of the dome as a function of time and allows a very quick and easy determination of the biaxial yield curve.

The yield curves from the bulge test lead to a considerably higher degree of deformation (up to 6 times higher) than that can be achieved in the standard tensile test. Therefore, the bulge test combined with the online strain measurement system ARAMIS provides an excellent new testing method for providing material data for a more effective numerical analysis.

This publication reviews the initial developments, outlines the main principles and influencing factors, presents the exemplary results achieved thus far and describes ongoing development activities.

Keywords: Yield Curve; Yield Surface; Bulge Test; Forming Simulation; Optical Strain Measurement

1. INTRODUCTION

Yield curves describe a material's work hardening behavior during forming and are therefore indispensable for FE forming simulation. The tensile test is used as initial test to fit the parameters of the different equations used to describe the yield curve. Since multiaxial stress states are present in most industrial forming processes, larger strains are required in FE simulation than those reached in the standard tensile test. The different equations used to describe the yield curves are therefore used in an extrapolated condition and do often not fit exactly with reality at large strains. Hocket-Sherby and Voce, for example, are underestimating the stresses at higher strains while Hollomon, Gosh and Swift-Krupskowski are overestimating them slightly and often the form of the curve does not fit well with the test data (Figure 1). A variety of different equations [1] and weighted sum of equations were proposed but the requirement for better experimental stress-strain curves is still very high because extrapolation leads to significant uncertainties.

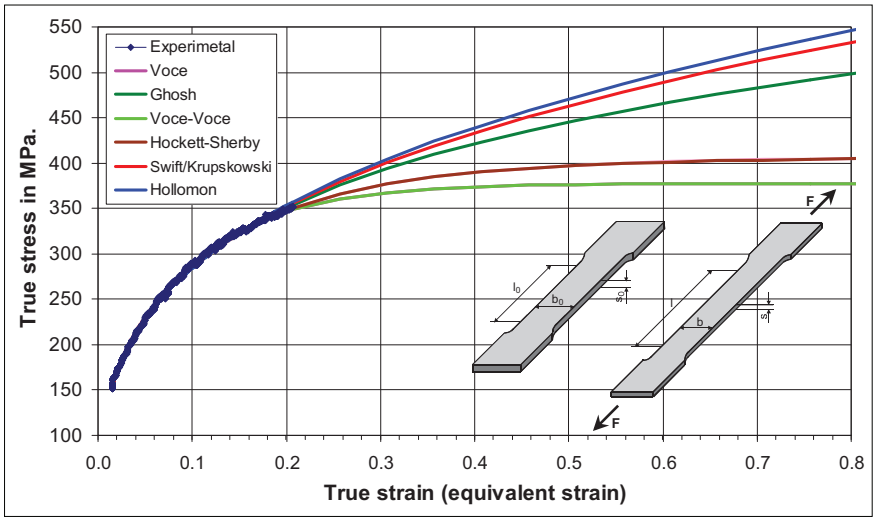

***Figure 1**: Measured and extrapolated yield curves from tensile test*

The relatively low strains reached in the tensile test can be explained by the uniaxial tensile state, which reduces the possibility of uniform deformation and of stable necking. If a biaxial stress state test is used, yield curves can be determined to far higher deformations in experiments and less or no extrapolation is therefore required.

An "in plane" biaxial test experiment is very difficult to set up, since the application of mechanical forces in both directions and in the plane of stresses at the same time is very complex. It is possible to use an out-of plane solution by limiting the thickness of the material with respect to its curvature, so that, in a first approximation, the stresses and strains are not changing across the thickness and both stresses are in the local plane (i.e. in the direction of the first derivative). This is the case in a bulge test where the thickness of the material is small with respect to the diameter of the die. A further advantage of the bulge test is that there is no friction since the force is transferred through fluid pressure.

When the pressure of the fluid p, the radius of curvature ρ, the local thickness t and the local strains ε_i are know, it is possible to determine the corresponding biaxial membrane stress using the equations given in Figure 2 [2]:

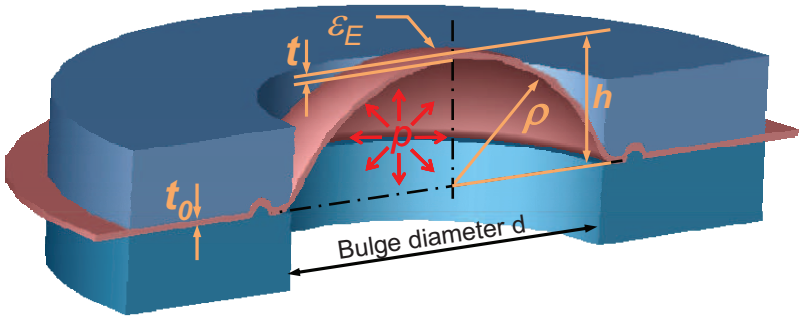

$$\sigma_b = \frac{p \cdot \rho}{2 \cdot t}, \quad t = t_0 \cdot \exp(-\varepsilon_1 - \varepsilon_2), \quad \varepsilon_E = \sqrt{4/3 \cdot (\varepsilon_1^{\,2} + \varepsilon_1 \cdot \varepsilon_2 + \varepsilon_2^{\,2})}$$

h	=	Dome height
p	=	Fluid pressure
ρ	=	Radius of curvature
t_0	=	Initial thickness
t	=	Actual thickness
ε_1	=	Major strain
ε_2	=	Minor strain
ε_E	=	Equivalent strain at the apex of the dome
σ_b	=	Bi-axial flow stress

Figure 2: *Extended bulge test used for yield curve determination.*

In the past, the determination of the curvature was carried out using of tactile mechanical sensors. The height was measured in three points and, using the height of the dome the local strains and the thickness were calculated (not measured) very approximately. The tactile three-point determination of the curvature is, however, not enough precise to give values with acceptable scatter. Even small variations of the measured height can lead to large variations in the radius determined by the three points.

A solution which makes use of optical online strain measurement systems such as ARAMIS results in a much better determination of the local curvature, thickness and strain. The degree of uncertainty is greatly reduced by measuring a very large number of point coordinates on the sample's surface during forming to track the specimen's local radius of curvature and its change in time accurately. The strains in and around the position to be analyzed are therefore determined precisely.

2. MATERIALS

In the present publication the following materials are investigated:

- Non heat treatable aluminum alloy AA5xxx in H111 temper
- Heat treatable alloy AA6xxx in T4 temper
- Dual-phase steel HCT600 XD
- Microalloyed steel H260LAD

3. EXPERIMENTAL PROCEDURE

3.1 Optical measuring system ARAMIS

For the measurement of the radius (curvature) and the strain values the measuring system ARAMIS [3] was used. A typical sensor (two cameras and a light source) is shown in Figure 3. A stochastic or regular pattern is applied to the specimen's surface and synchronized stereo images of the pattern are recorded at different loading stages.

Figure 3: *ARAMIS sensor with light source for FLC and bulge tests*

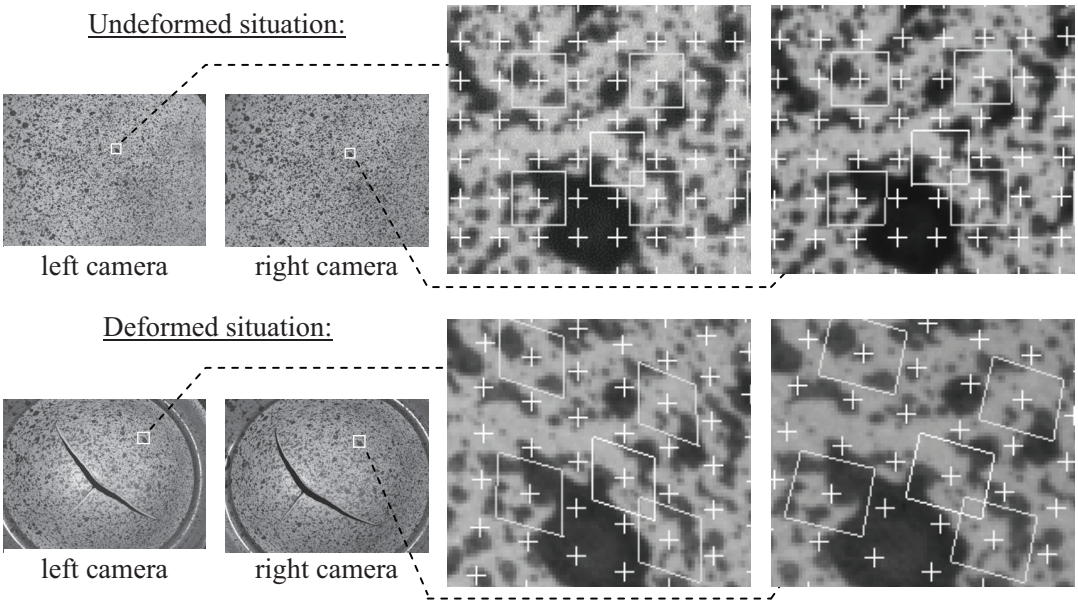

Figure 4: *Typical measurement images: left side full image size, right side enlarged local area with mathematical subsets (facets) for the calculation of surface point.*

Figure 4 shows the undeformed and the deformed situation for a specimen. In this case the image of the undeformed situation of the left camera is divided into a large amount of subsets (facets). The center of each facet is shown as a cross, five of the facets are shown as quadrangle. For each face the corresponding area is calculated for the right camera also for all loading stages. Based on the well known geometry of the optical setup for each center of a facet (each cross in Figure 4) a 3D point is calculated for all loading stages and for each point following result values are e.g. derived:

- 3D coordinates displacements and speeds
- Surface strain tensor (strain x, -y, xy, major, minor, thinning) and strain rates

The usability of this system for determining the materials flow curve was tested by measuring a plane and stiff reference plate (size 100 mm x 80 mm) in different displacement conditions. The reference plate was moved towards the measuring system in multiple steps (see displacement results for a cross section in Figure 5 left side). The displacements are large, so that the deviation can not be recognized in this diagram. The values in Figure 5 right side are calculated by subtracting the rigid body motion from the displacement results. These values show, that the deviation in the geometry based on stochastical and systematical influences for this ARAMIS measurement are in the range of ±2 µm.

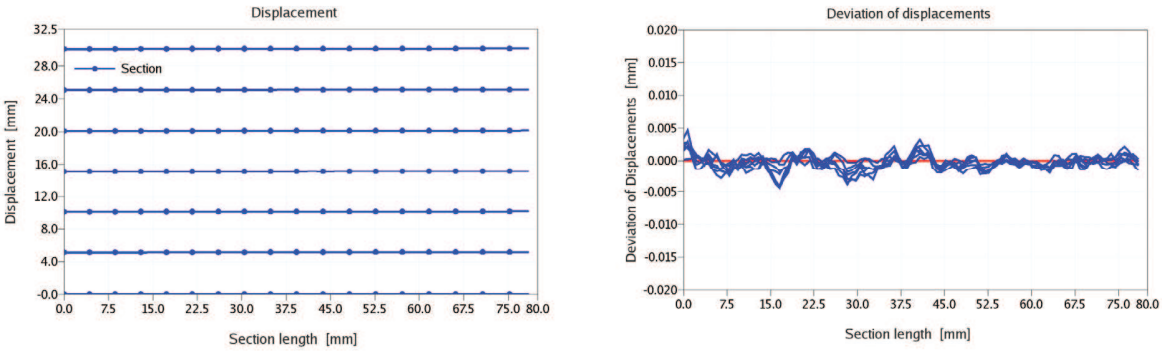

Figure 5: *Displacement results for a rigid body movement test with a reference plate. Left side original displacements for a cross section, right side deviation after rigid body movement compensation.*

3.2 Description of the test equipment

In order to achieve reproducible results, the geometry of the bulge test rigs in the different laboratories should be as close as possible with regard to key dimensions. The diameter of the used die is 100 mm and corresponds to the geometry used for FLC determination (Figure 6). The oil pressure is built up with a pressurized piston and the acting pressure is directly measured in the cylinder to eliminate errors caused by friction between piston and cylinder.

The configuration of the ARAMIS system corresponds with that used for FLC determination, but instead of the mechanical punch, oil pressure is used to deform the specimen.

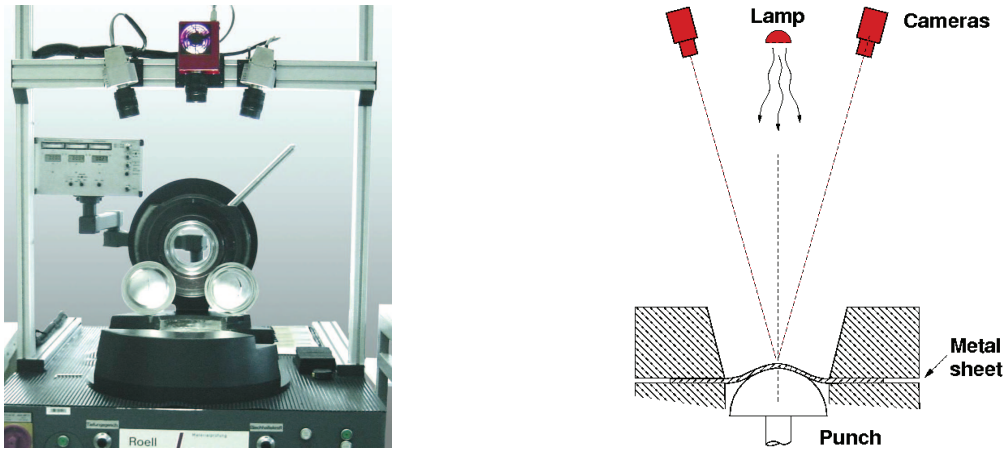

Figure 6: *Test equipment for FLC.*

To protect the CCD cameras and the light source from splashing oil when the specimen bursts a special shield construction consisting of transparent and non-reflecting windows should be used in any case. The protective glass plates in front of the cameras lens and light source has to be positioned perpendicular to the optical path and as near as possible to the lens so that no distortions and no unintended reflections are caused by the glass plates. In this position, the glass plates are far away from the focus point of the lens and any eventual reflections are blurred and minimized (Figure 7). The glass plates have to be of optical quality but do not need to be very thick since the distance to the bursting sample is quite long.

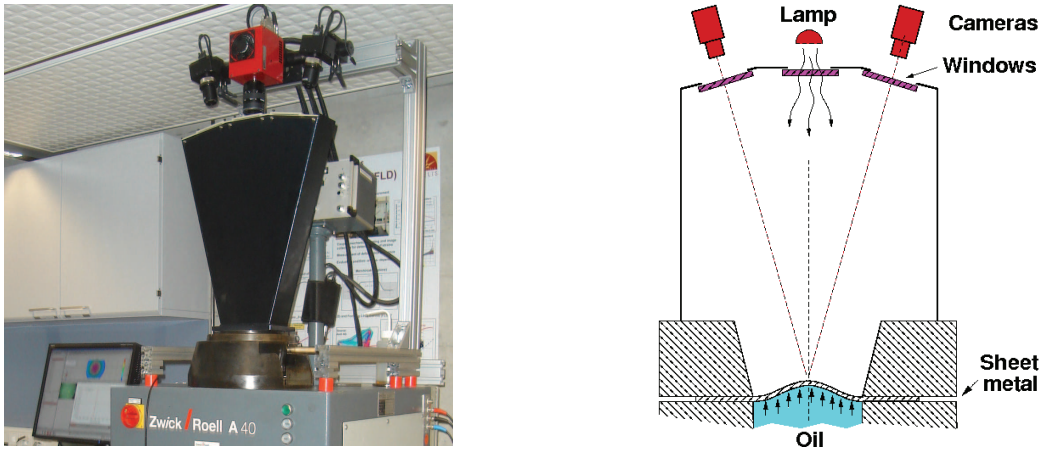

Figure 7: *Protection of cameras and light source from splashing oil at the moment of burst.*

The ARAMIS system is mounted, focused and calibrated. The pressure measurement signal is connected to ARAMIS and the pressure value registration is triggered to the instant the images are taken.

3.3 Measuring procedure

- The cylinder over the piston is filled with oil completely so that no air remains in the pressure chamber. Since air is compressible the stored energy can lead to a stronger burst at the moment of fracture.
- The sheet disc or blank is clamped into the bulge test rig.
- The shielding unit which protects the cameras and the light source are positioned.
- The piston speed is set to about 1 mm/sec
- The first image is taken before starting the test and is used as the undeformed reference for the strain calculation.
- During the test, image pairs together with the corresponding pressure are recorded at defined time intervals (10 times/sec) until the sheet bursts.
- After each test, the transparent shields have to be cleaned carefully.

3.4 Evaluation procedure

Based on the resolution of the camera and the mathematical parameter for the facets for these tests (using a camera with 1.3 MPixel) a typical local distance between adjacent points of about 1 mm is used.

On the last image before bursting the area at the apex of the dome with the highest deformation is selected and defined as position where to determine the stress and the equivalent strain ε_E in ARAMIS. Based on the formula given in Figure 2 for this point also the radius of curvature and the thinning are calculated.

For getting a stable radius of curvature in the apex of the dome in ARAMIS a best fit sphere can be calculated based on a selected area of points. For this selection in the last image before bursting a radius R1 is defined around the apex of the dome (Figure 8) and the fit is done for all forming stages with the same selection of points (Figure 9).

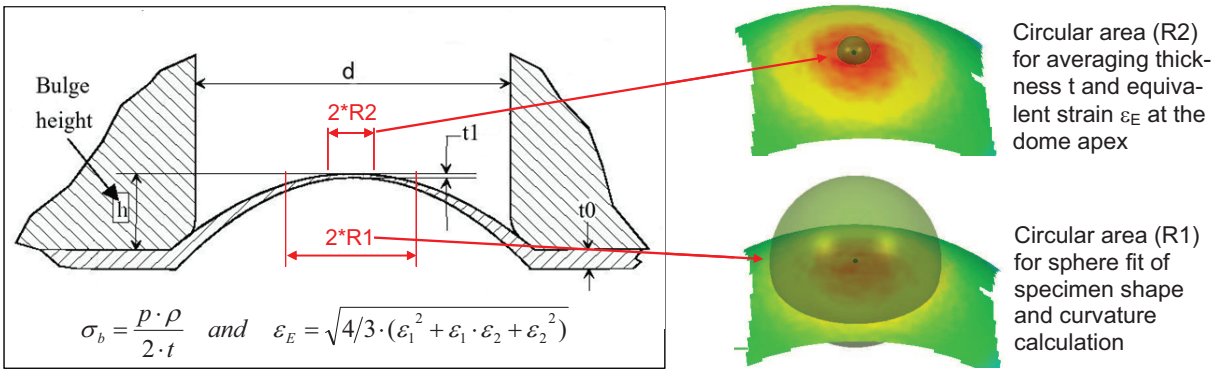

Figure 8: *Choice of R1 and R2 for calculation of true stress and true strain for each forming stage [4].*

A certain number of the first images are rejected, since the specimen is still too flat for a reliable determination of the best fit sphere, since the bending radius is very high and the fit is not stable. To get robust values for the strain and thinning in the apex, the average of a number of selected points is taken. Therefore a second area is defined by radius R2 in a similar manner (Figure 8).

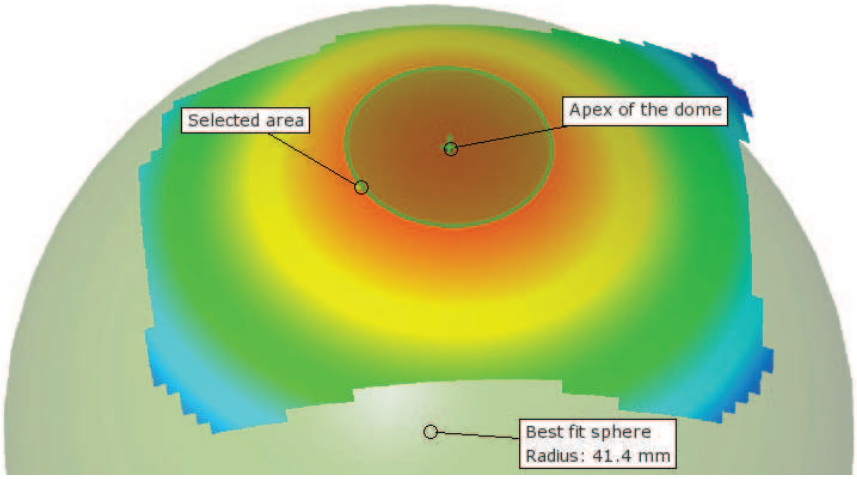

Figure 9: *Best-fit sphere based on the contour values of an area defined by R1 around the apex of the dome*

Based on this procedure, ARAMIS calculates for every forming stage (image) the radius of curvature, thickness and equivalent strain at the dome apex and the corresponding strain and stress values. This evaluation can be carried out for different R1 and R2 values in an easy way.

4 EXPERIMENTAL RESULTS

4.1 Parameter study of R1 and R2

Within the parameter study the radius R1 (= area for radius of curvature calculation) was varied between 7 and 40 mm and, as can be seen in Figure 10, a good convergence in the course of the determined yield curves can be achieved with an R1 value of 17.5 mm. Therefore the recommended R1 value for the calculation of the specimen curvature by means of a best-fit sphere is about 17.5 mm.

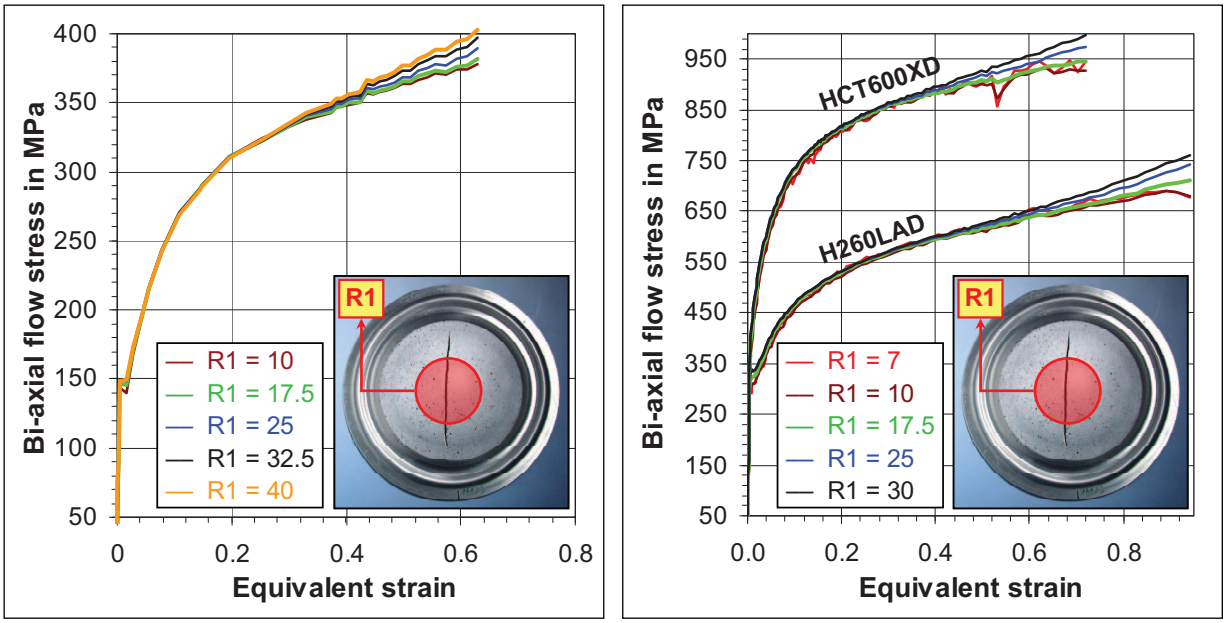

***Figure 10**: Influence of radius R1 on the yield curve course*
a) Aluminum alloy AA5xxx *b) Steel HCT600XD and H260LAD [4]*

An optimized method is to start with a larger radius (e.g. 25 mm) at the beginning of the test when the radius of curvature is large. With ongoing deformation the radius has to be reduced to a smaller value of between 10 and 12 mm to get a better best-fit sphere when the radius of curvature becomes smaller. The Radius R1 can be optimized by minimizing the residuals of the fit. Further optimization, for example, could be achieved in future by using a paraboloid instead of a sphere and will be subject of further investigations.

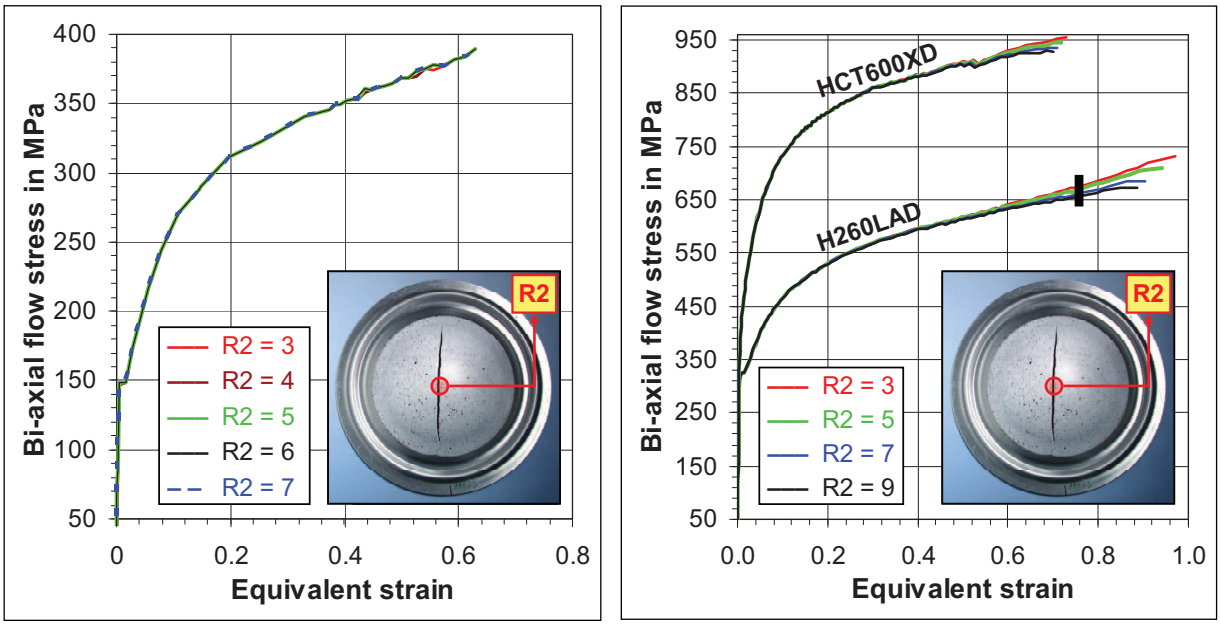

***Figure 11**: Influence of radius R2 on the yield curve course*
a) Aluminum alloy AA5xxx *b) Steel HCT600XD and H260LAD [4]*

To determine robust values for thickness and equivalent strain at the apex of the dome the average of an area defined by R2 is used (Figure 8). In the present parameter study, values of between 3 and 9 mm were investigated. For equivalent strains up to 0.75, there is no significant influence of the chosen radius on the course of the biaxial yield curve (Figure 11).

For materials with higher degrees of deformation (Figure 11b) the deviations between the set of curves are increasing up to 5% for strain values higher than 0.75. Based on these investigations a value for radius R2 of about 5 mm is considered to be most suitable for the determination of thickness and equivalent strain at the dome apex.

4.2 Small round-robin test

Using the above-described procedure and a preliminary standardization of the testing and evaluation parameters, a small round-robin between Hydro, Novelis and in part IVP Zürich was carried out. The resulting curves displays very little scatter, which demonstrates a good inter-laboratory reproducibility **(Figure 12)** although different testing machines and die geometries were used.

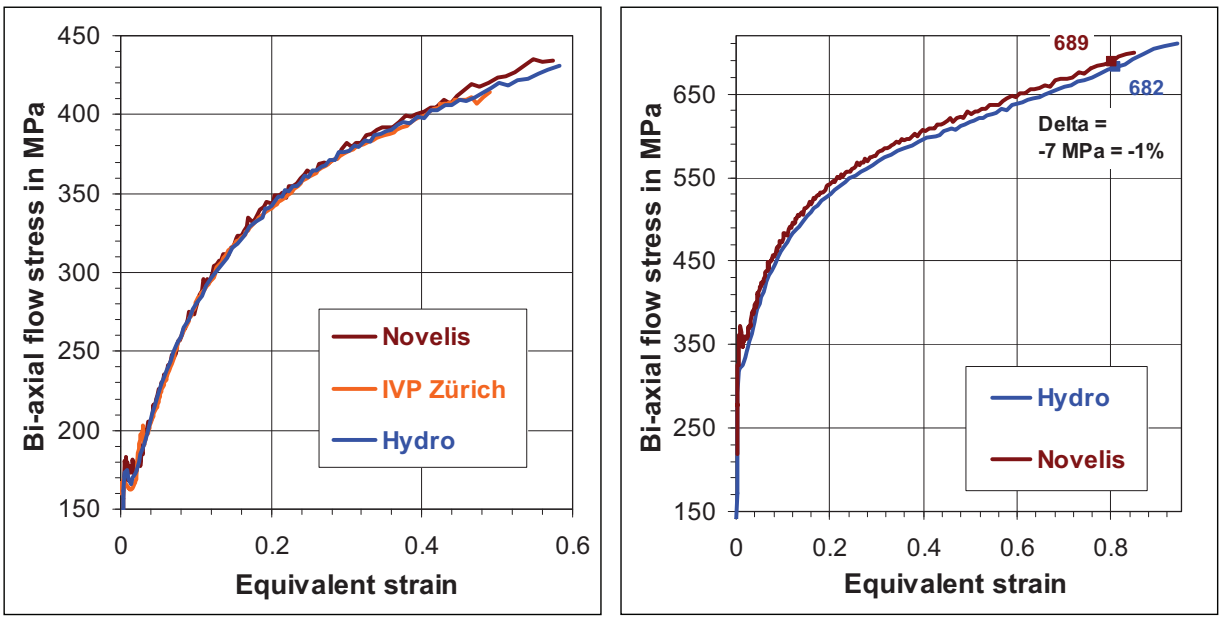

Figure 12: *Comparison of biaxial flow curves measured in different laboratories*
a) Aluminium AA5182, 1.05 mm, H111 temper *b) H260LAD, 0.995 mm [5]*

Based on these results, it can also be stated that the camera's protective shielding as described above does not have an influence on the results if the ARAMIS system is calibrated with the shielding glasses.

4.3 Exemplary results for different materials in comparison with tensile test

In the following Figures (13-15) exemplary results for different alloys and tempers are shown. It can be seen that yield curves from the bulge test lead to a considerably higher degree of deformation than can be achieved in the standard tensile test (even up to 6 times higher).

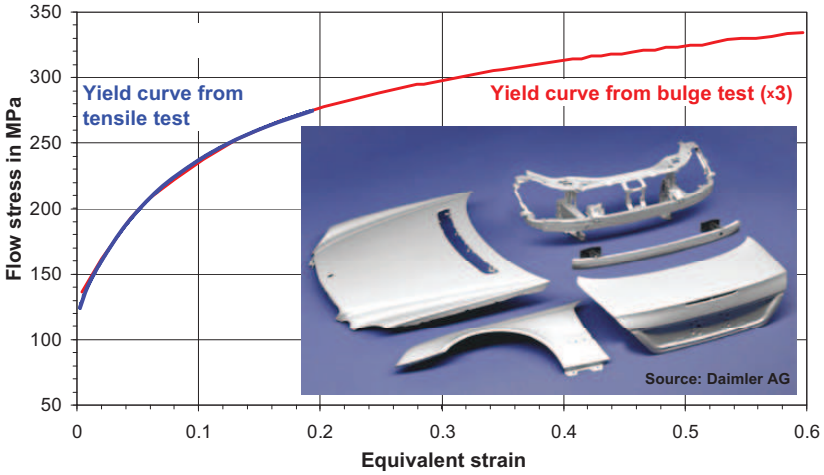

Figure 13: *Yield curve form tensile and bulge test for car body outer panels (AA6xxx) in T4 temper*

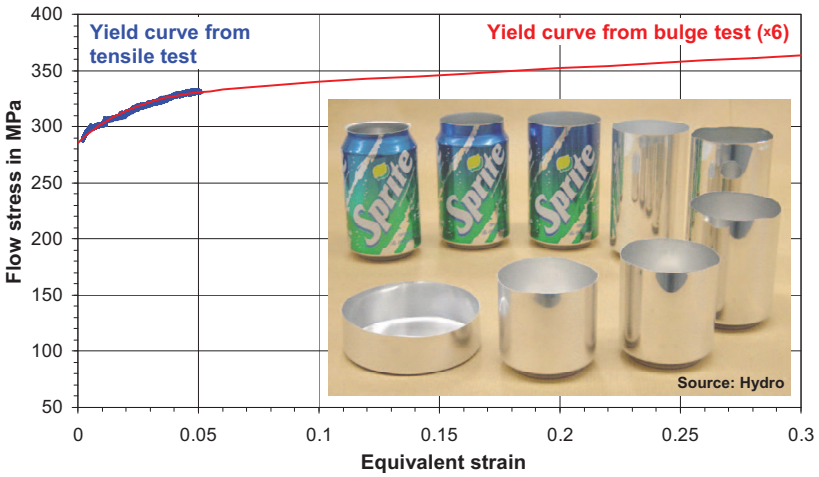

Figure 14*: Yield curve form tensile and bulge test for can stock (AA5xxx) in as rolled temper (H19)*

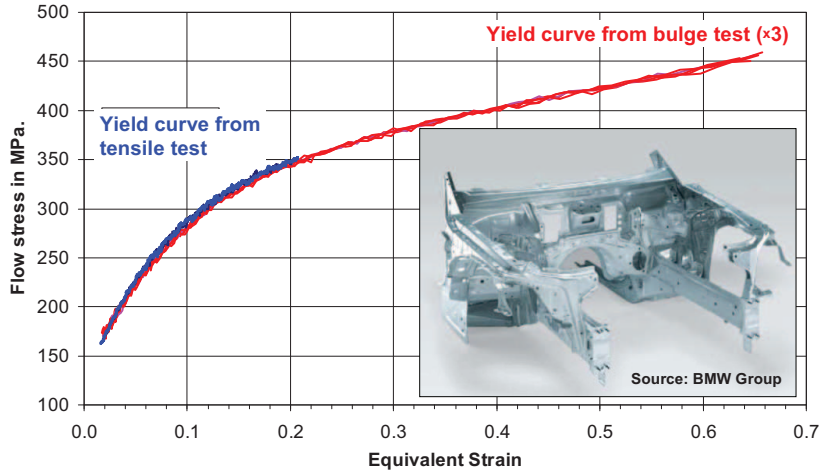

Figure 15*: Yield curve form tensile and bulge test for test for car body inner panels AA5xxx [6].*

5. DISCUSSION OF RESULTS

Figure 16 shows fitted yield curves, based on different equations and experimental data (left side from tensile tests and right side from biaxial bulge test). It can be clearly seen that the curves based on the biaxial bulge tests match the experiment much better and the scatter between the different fitted and extrapolated curves is less. The strain values achieved in bulge test are so high that an extrapolation is no longer necessary in most cases.

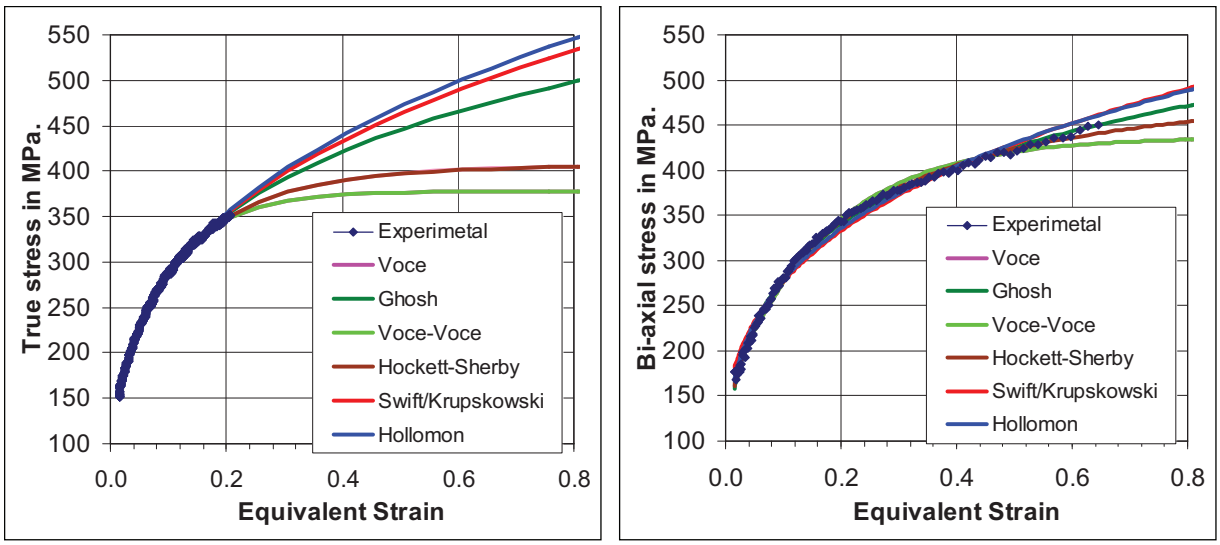

Figure 16: *Comparison of yield curve equations fitted from tensile and from biaxial flow stress tests (AA5182-H111, 1.05 mm)*

6. SUMMARY AND CONCLUSIONS

- Yield curves (true-stress vs. true-strain curves) describe a material's work hardening during forming and are thus indispensable for all FE forming simulations.
- As a well known fact, the biaxial bulge test leads to considerably longer yield curves (even up to 6 times) than those achieved in the standard uniaxial tensile test.
- For simplifying the biaxial yield-curve measurement and achieving significantly improved accuracy, GOM, Hydro and Novelis established a joint venture in 2004 and combined the old-fashioned bulge test with a modern online strain-measurement system.
- This system includes the measurement of pressure, dome height, dome curvature and equivalent strain at the apex of the dome as a function of time.
- This combined Bulge-Test/ARAMIS System allows a quick and accurate determination of the biaxial yield curve which, for example, can be used for the following purposes:
    - Quality assurance of ongoing production
    - Comparison of the work-hardening behavior of different materials
    - Provision of reliable yield curves for more effective numerical analysis of material behavior in forming processes
- An interim standardization procedure for the testing and evaluation parameters was worked out and leads to reproducible results in different laboratories.

7. FUTURE WORK

- Continuation and extension of the above mentioned standardization work and preparation of an ISO proposal within the German IDDRG "Bulge Test" Working Group launched in July 2007 (Figure 17).
- Implementation of more robust regression approaches for the specimen's curvature determination, e.g. sphere fit area with varying radii or paraboloid fit instead of a sphere fit.
- Improving the method for transforming the measured biaxial yield curves into a uniaxial stress state required by FE software.
- Extension of the method to the determination of the onset of plastic flow in an equibiaxial stress and the biaxial anisotropy value (r value), both required for a better description of the yield surface.

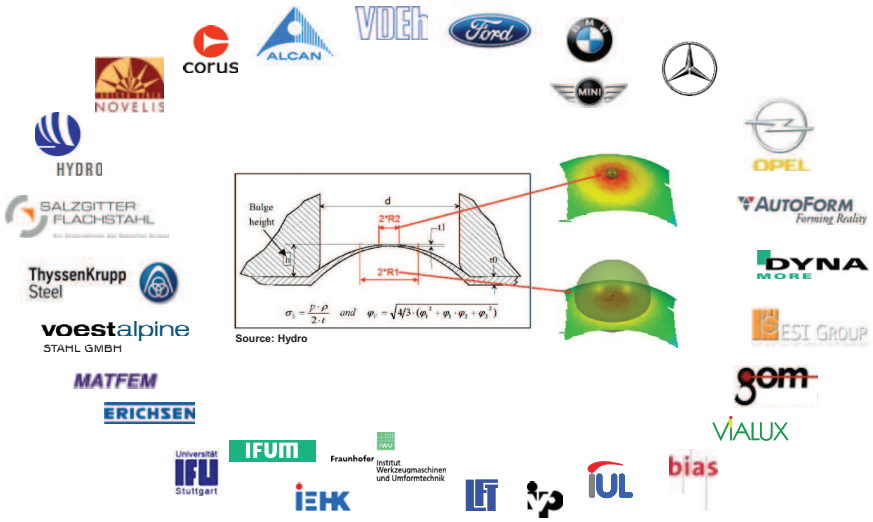

Figure 17: *IDDRG – German Working Group „Bulge Test"*

8. BIBLIOGRAPHY

1 H. J. Kleemola and M. A. Nieminen: "On the Strain-Hardening Parameters of Metals", Metallurgical Transactions, Volume 2, 1974, 1863

2 F. Gologranc: Beitrag zur Ermittlung von Fließkurven im kontinuierlichen hydraulischen Tiefungsversuch, Berichte aus dem Institut für Umformtechnik, Universität Stuttgart, Nr. 31 (1975), Verlag W. Girardet, Essen

3 H. Friebe: "Kennwertermittlung und Verifikation von Umformsimulationen mittels optischer Messverfahren", Tagung Werkstoffprüfung 2006, "Fortschritte der Kennwertermittlung für Forschung und Praxis", Verlag Stahleisen, Düsseldorf, 2006, 239-244

4 S. Keller: "Einflussgrößen beim Bulge-Versuch und deren Auswirkung auf das Ergebnis (Influencing parameters in bulge testing and their effects on the results)", German IDDRG Group, meeting minutes of the "Bulge-Test" working group, May 2008.

5 S. Keller, W. Hotz, C. Leppin: "Vergleich der Ringversuchsergebnisse von Novelis/Alcan, Hydro und IVP Zürich (Comparison of the Round-robin test results from Novelis/Alcan, Hydro and IVP Zürich)", German IDDRG Group, meeting minutes of the "Bulge-Test" working group, May 2008.

6 W. Hotz, J. Timm: "Biaxiale Fliesskurvenbestimmung bei Novelis (Determination of biaxial flow stress curve at Novelis)", German IDDRG Group, meeting minutes of the "Bulge-Test" working group from 17.07. 2007.